Selective reflection by Rb

Ping Wang, A. Gallagher, and J. Cooper
JILA, National Institute of Standards and Technology and University of Colorado, Boulder, Colorado 80309-0440
(Received 8 January 1997)

Perpendicular reflection of low-power, near-resonant radiation at a sapphire–Rb-vapor interface (selective reflection) has been measured for Rb densities of 3×10^{14}–$3\times10^{17}/\mathrm{cm}^3$. At the lowest density the eight hyperfine components are essentially isolated, and at the highest pressure they are highly blended. The data have been fitted to a coherent superposition of the reflected field amplitudes of the eight components, including the well-known starting transient and wall interaction. At low to moderate densities this yields a good fit to the data, and a result for the Rb-Rb collisional shift. At the higher densities the rapid attenuation of the incident field has a major effect on the reflection spectrum, and an approximation to this is included in the calculation, assuming exponential attenuation at the equilibrium-vapor rate. This provides improved fits to the data and allows the apparent Lorentz-Lorenz plus collisional shift to be evaluated. However, the data do not fully fit this calculation, and a complete self-consistent-field calculation appears necessary to fully understand the high-pressure results. [S1050-2947(97)06108-8]

PACS number(s): 42.50.Fx, 32.70.Jz

I. INTRODUCTION

Selective reflection (SR) refers to the enhanced reflection that occurs at a window-vapor interface for light tuned near the atomic resonance line. Many aspects of this phenomenon have now been studied, stimulated by Schuurmans and Woerdman's demonstration that it contains a sharp reflection feature at the resonance frequency [1]. This feature results from the fact that atoms leaving the window surface are suddenly immersed in the radiation field, and thereby undergo a transient oscillation at the resonant frequency. SR has been measured versus incident radiation angle [2], versus power, including sufficient power to optically pump the atom [3,4], using independent pump and probe frequencies [5], with an antireflection coated window [6], using an evanescent wave [7], and at high and low vapor densities (N). All measurements have used alkali resonance lines.

The theory for the expected wavelength-dependent SR is fairly straightforward for an isolated line and low-power radiation [1,8,9], but is not easy to evaluate without approximation. The most common approximation is to assume a sufficiently low N that the incident field is not significantly attenuated within the spatial region near the window in which the atomic transient decays away. Ducloy has even obtained analytic expressions for many reflection properties within this approximation [10]. Using this approximation, an excellent understanding of many characteristics of SR have been achieved, including the effect of the atom-wall van der Waals interaction [8,10]. However, most SR measurements are not made in this regime, since the signal size grows rapidly with N. At high N, the field attenuation length on resonance becomes almost the same as the transient decay distance, and one expects significant corrections to the low-N calculations. The emphasis of this paper is on these differences between the low and high density cases, and the data reported here transverse the entire density regime between these limits.

The SR feature is characterized by a homogeneous linewidth, of $\Gamma+2\gamma^c$, the natural plus collisional width, hence SR can be used to measure collisional broadening. It is particularly useful for measuring self-broadening, since this normally requires a high vapor density and the resulting rapid attenuation of resonance radiation precludes using alternate techniques such as saturated absorption. In principle, the self-broadening collisional shift can also be measured by SR, but a number of other phenomena also contribute a shift of the apparent resonant frequency. The van der Waals interaction between atoms and wall causes a redshift [8], and the Lorentz-Lorenz self-field correction to the local field causes a ''Lorentz-Lorenz'' redshift [11]. In addition, a recent calculation has shown that the reflection is further altered by nonexponential field attenuation and by hyperfine component partial overlap with the Doppler envelope [12–14]. Finally, calculations reported here, which include the rapid field attenuation at high N, demonstrate a resulting shift. Some SR studies have reported measurement of the collisional shift, but without accounting for all of these contributes to the SR shift [15,16]. Here we also study the shift, across the large-N range of our data, and compare it to calculations based on various levels of theoretical approximation.

Most measurements of SR have concentrated on situations where different hyperfine peaks were relatively isolated in the SR spectrum, and then interpreted these as isolated lines [16]. In the other limit, Maki and Boyd measured SR at high K densities, where the homogeneous width was much larger than the hyperfine structure (hfs) and they could consider it as a single line [15]. Here we measure the full spectrum of eight Rb hyperfine components, from low densities where they appear isolated to high densities where they are blended into a single SR feature. We compare this to the appropriate coherent superposition of eight reflected field amplitudes, thereby achieving comparisons for all amounts of overlap. However, since fully self-consistent calculations are numerically challenging and have yet to be fully implemented, we do not use a self-consistent field in the vapor. As will be seen this results in significant line-shape discrepancies and difficulty in accurately determining the collisional shift.

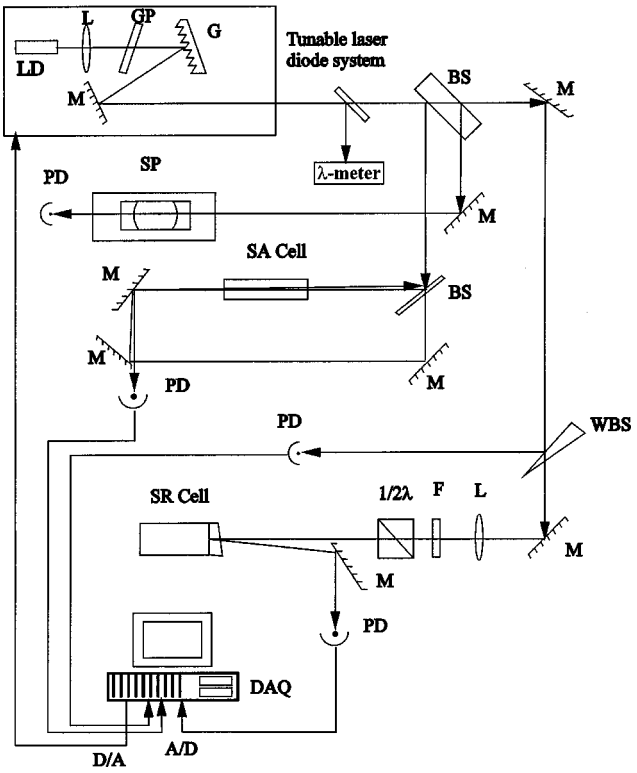

FIG. 1. Experimental setup. LD: laser diode; L: lenses; GP: galvo plate; SP: spectral analyzer; G: blazed grating; M: mirrors; BS: beam splitter; PD: photodiodes detectors; F: filter; 1/2λ: half wave plate; DAQ: computer data acquisition system; SA: cell is rubidium cell at room temperature; SR cell is a heated rubidium cell.

The experimental details are described in Sec. II, the theoretical expressions and approximations used for comparison to the data are in Sec. III, the data and comparisons to the calculations are in Sec. IV, and the conclusions are in Sec. V. The thesis of Ping Wang provides many details that are not presented here [17].

II. EXPERIMENT

A ~2-mm-diameter beam from a tunable diode laser was reflected, within 2 mrad of perpendicular incidence, from the vapor interface of a wedged sapphire window of a Rb vapor cell. Figure 1 shows the optical scheme for the experimental setup. A grating-feedback cavity, tunable laser-diode system provides a narrow linewidth (<1 MHz) laser beam, tunable with a galvanometer-mounted Brewster plate. One laser-beam component went to a low-pressure, Rb saturated-absorption cell to provide the frequency reference for the SR signal, a second component provided an intensity reference, and a third provided the SR signal after reflection. Another component to an interferometer provided mode structure and scan data used to correct for a few percent scan nonlinearity. The SR signal is expressed as $R' = \Delta R/R$, where R is the off-resonance reflection at the window-vapor interface (~7%) and ΔR is the reflectance change due to the Rb vapor. Frequency scans of ~500 steps and several minutes were normally used, and after division of the SR signal by the intensity reference, the fluctuations in R' were typically 10^{-4}.

The Rb cell used a 2° wedge sapphire window fused to a 0.5-in.-diam polycrystalline-alumina (PCA) tube, which was fused to a smaller PCA tube that was fused to a ~6 mm-diam kovar tube with a 5° taper joint. The kovar tube was welded to a stainless-steel tube, and thereby connected through nickel-gasketed standard stainless-steel vacuum fittings to a high-temperature stainless-steel valve and a turbomolecular pump. All fused joints were made with a high-temperature sealing frit, following the procedures outlined in Ref. [18]. The laser beam incident on the cell was linearly polarized, and aligned with a polarization-preserving axis of the sapphire window.

The cell and hot valve are maintained 5–20 °C above the temperature (T) of the Rb reservoir at the middle of the stainless tube. T was controlled within 0.1 °C by a servo controller, but the accuracy of T is ±2 °C over the temperature range studied (125 °C–425 °C, corresponding Rb density of 3×10^{13}–2.7×10^{17} cm^{-3}). The Langmuir-Taylor relation [19] at T was used to establish the Rb density. Due to the uncertainty in T and in the Langmuir-Taylor relation [20], the accuracy of this vapor density is typically ±20%. As will be shown, the SR signal yields the density with somewhat improved accuracy.

The Rb vapor does not affect the sapphire window within our experimental temperature range. Even if Rb condenses onto the window, increasing the window temperature removes it without leaving a stain. When the cell is heated to >275 °C, the sealing glass is slowly corroded by the hot, dense rubidium vapor. Part of the transparent glass joint between sapphire window and PCA first turns yellow, and eventually is etched through and starts to leak. However, the cell can last more than 500 h in the range 275 °C–425 °C.

III. THEORY AND EXAMPLES OF SELECTIVE REFLECTION

The theory of low-intensity SR from a low-density vapor of two-level atoms is well established [1,8,9]. Here we extend this to the present conditions of overlapping hyperfine components and higher densities. We start from the established theoretical models for low vapor density, which include the atom-wall interaction [8,9]. We will add an exponential-decay approximation and overlapping line effects. We note the effect of the Lorentz-Lorenz self-field correction, but include it only as a shift. A full theory must use self-consistent field attenuation in the vapor plus the Lorentz-Lorenz correction explicitly. This has been done for certain specific parameters in Refs. [12–14], but at the present time this would require excessive computation time for the conditions explored here.

The atomic vapor is contained in the $z>0$ region, with the interface in the x-y plane. A linearly polarized light beam is normally incident on the interface from the dielectric medium toward the vapor, and is partially reflected back into the dielectric medium. The intensity of the reflected beam is monitored as a function of the frequency of the incident light. The refracted beam in the vapor interacts with the atoms, influencing the reflected function when tuned near the atomic resonance line.

Including the Lorentz-Lorenz self-field correction and the C_3/z^3 atom-wall interaction [8,10], the interaction energy

term of the Hamiltonian for the two-level atoms in the radiation field is

$$V_{\rm int}=-\mathbf{d}_{21}\cdot\left[\mathbf{E}(z)+\frac{4\pi}{3}\mathbf{P}(z)\right]-\frac{\varepsilon-1}{\varepsilon+1}\left[\frac{d_{21}^2+d_{21_z}^2}{16z^3}\right]. \quad (1)$$

Here $\mathbf{E}(z)$ is the total field, $\mathbf{d}_{21}$ is the transition dipole moment in terms of the polarization in the medium $\mathbf{P}(z)$, $\varepsilon=n_w^2$ is the dielectric constant, and n_w is the index of refraction of the window, the second term is the origin of the Lorentz-Lorenz shift and the last term is the London–van der Waals, surface-interaction potential. Hence, C_3 an attraction strength of the London–van der Waals potential is defined as

$$C_3=-\frac{\varepsilon-1}{\varepsilon+1}\frac{[\langle n|d^2+d_z^2|n\rangle-\langle g|d^2+d_z^2|g\rangle]}{16h}, \quad (2)$$

where $|g\rangle$ and $|n\rangle$ refer to the ground and excited states, respectively. For simplicity, a dimensionless coupling constant C, which measures the surface-induced frequency shift is introduced as

$$C=\frac{2C_3}{\lambda^3\gamma_2}, \quad (3)$$

where λ is a reduced wavelength and γ_2 is a natural linewidth of the excited state. Using a hydrogenic model, with effective principal quantum numbers of 1.805 and 2.292 for the Rb $5S_{1/2}$ and $5P_{1/2}$ states, and $n_w=1.76$ for sapphire at 795 nm, this results in $C_3=1.2$ kHz(mm)^3, corresponding to $C=0.2$ [17]. This calculated C value applies to all hyperfine components due to an effective isotropy assumption. (Ducloy and co-workers have used a more exact method to calculate the surface potential strength C_3 of several Cs transitions. To check for differences between the two methods, we calculated these C_3 using the hydrogenic model and found agreement within 10%.)

The two stable isotopes of rubidium, Rb^{85} and Rb^{87} with abundances (A_n) of 72% and 28% and $I=5/2$ and 3/2, yield eight components of the Rb D_1 line spread across ~8 GHz. Some of these overlap within the Doppler envelopes, and due to line broadening they all overlap within the homogeneous width at the higher densities studied here. If optical pumping is not significant, as assumed here, the relative transition strength of the $F\rightarrow F'$ hyperfine structure component is

$$g_{F'F}=\frac{(2F+1)(2F'+1)}{2I}\begin{Bmatrix} F & J & I \\ J' & F' & 1\end{Bmatrix}, \quad (4)$$

where F (F') is the total angular momentum of the excited (ground state).

We assume an exponentially decaying field in the vapor, with attenuation coefficient $\alpha(\Delta)$ equal to that of the vapor without a wall transient:

$$E(\Delta,z)=\frac{2n_w}{n_w+1}E_i\exp(ikz-\alpha(\Delta)z], \quad (5)$$

where E_i is the amplitude of the linearly polarized incident field at the interface,

$$\alpha(\Delta)=\sum_{i=1}^{8}\alpha_n(\Delta_n)=\sum_{i=1}^{8}3\pi^{3/2}\left(\frac{\gamma_2}{2ku}\right)(g_nNA_nk^{-3})I\left(\frac{i\gamma_{21}+\Delta_n}{ku}\right)k, \quad (6)$$

where N is the density of the Rb vapor and A_n is the abundance of Rb isotopes, $I(z)$ is the error function associated with the Voigt line shape,

$$\gamma_{21}=\frac{\gamma_2}{2}+\gamma_{\rm self}+i\gamma_{\rm shift}, \quad (7)$$

$2\gamma_{\rm self}$ and $\gamma_{\rm shift}$ are the collisional broadening and shift due to collisions with identical atoms, and $\Gamma=2\gamma_{21}$ is the homogeneous width. Here k is the propagation wave vector, u is the mean thermal velocity, and $\Delta_n=\omega-\omega_n$ is the detuning of the laser frequency from the hyperfine component, g_n refers to the appropriate C-G coefficient, $g_{FF'}$.

The reflected field has been given by Refs. [1–3] for the low-density case; adding the above generalization but deleting the Lorentz-Lorenz correction yields the SR signal $\Delta R/R_0=(R-R_0)/R_0$ with

$$R=\left(\frac{E_r}{E_i}\right)^2=\left[\frac{n_w-1}{n_w+1}-\sum_{n=1}^{8}g_nA_n\Phi(\Delta_n)\right]^2, \quad (8)$$

where

$$\Phi(\Delta)=\frac{n_w}{(n_w+1)^2}\frac{8\pi kNd_{21}^2}{\hbar}\int_0^\infty\frac{dv_zW(v_z)}{v_z}\int_0^\infty dz\,\exp(ikz)\times\left\{\int_0^z dz'\exp[ik-\alpha(\Delta)]z'\exp\left[-\frac{\gamma_{21}-i\Delta}{v_z}(z-z')-\left(\frac{C_3}{2z^2}-\frac{C_3}{2z'^2}\right)\frac{1}{v_z}\right]+\int_{-\infty}^{z}dz'\exp[ik-\alpha(\Delta)]z'\times\exp\left[-\frac{\gamma_{21}-i\Delta}{v_z}(z-z')-\left(\frac{C_3}{2z^2}-\frac{C_3}{2z'^2}\right)\frac{1}{v_z}\right]\right\}, \quad (9)$$

and $W(z)$ is the Maxwellian vapor velocity distribution.

Although the line shape of Sr is altered by the Lorentz-Lorenz self-field correction, the primary effect is a shift of the entire line shape [13]. The collisional shift simply shifts the entire line shape, so for convenience we will delete the Lorentz-Lorenz correction and the collisional shift from the calculation, a major simplification, and assume that any shift between the calculated and measured Sr is due to the sum of these two shifts.

The SR signal is strongly influenced by the transient response of atoms that leave the window surface in the ground state and are suddenly immersed in a near-resonant field. In the low-density limit, the absorption of the vapor is sufficiently small that the field attenuation within the z region of atomic transient response is negligible. Deleting the field attenuation $\alpha(\Delta)$ and taking a single-component line, Eq. (5) reduces to those from Refs. [1,8,9] for low N. Equations

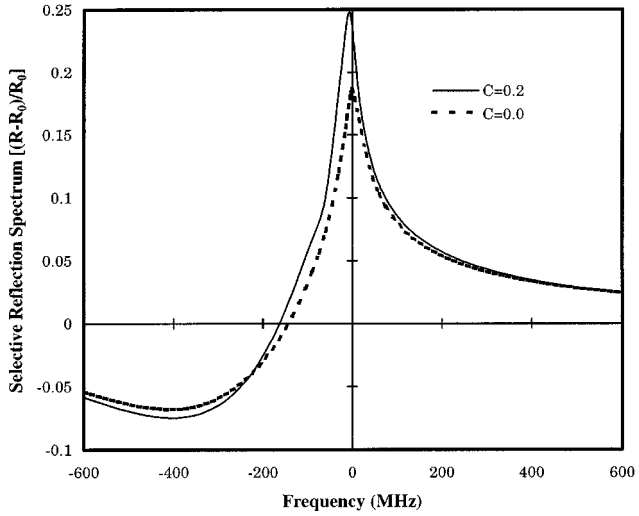

FIG. 2. Theoretical SR line shapes for the Rb D_1 line at 3×10^{14} cm^{-3} density, assuming no hfs isotope splitting. The dashed line is without the atom-wall interaction, with the solid line includes the wall interaction with $C=0.2$.

(1)–(9) will now be used to demonstrate the N dependence of various features of SR. We will start with a single-component line.

To demonstrate the effect of the wall interaction, the SR signal is compared for $C=0$ and $C=0.2$ in Figs. 2 and 3, using parameters for the Rb D_1 line ($5P_{1/2}\rightarrow5S_{1/2}$, $\lambda=7948$ Å) without hfs, and $N=3\times10^{14}$ cm^{-3} and 1.7×10^{17} cm^{-3} corresponding to Rb at $T=175$ and 400 °C. $R_0=0.076$ is the reflection coefficient on the absence of the vapor, the natural linewidth $\lambda_2/2\pi$ is 6 MHz, the Doppler width is $ku=62\gamma_2$ and the collisional self-broadening coefficient is $k_{br}=4.2\times10^{-7}$ s^{-1} cm^3 corresponding to resonance broadening of D_1 line transition of Rb atoms [21]. The SR signal shifts to the red and increases in size at all densities due to the atom-wall interaction. The red-shift is ~4 MHz at the lower N, which is characteristic of the low-density limit, to ~560 MHz at the higher N.

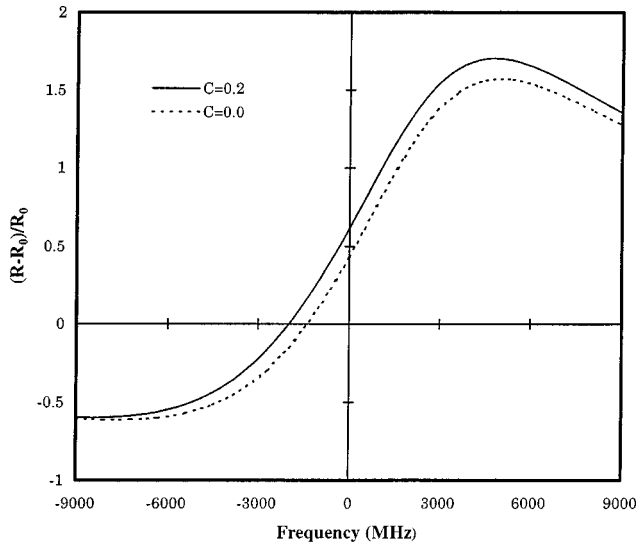

FIG. 3. Line shape of SR for the Rb D_1 line at atomic vapor density 1.7×10^{17} cm^{-3}, assuming no hfs.

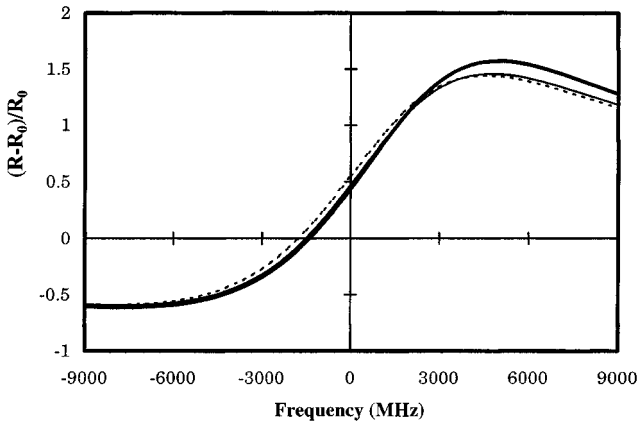

FIG. 4. Calculated Rb D_1 line shape of SR at atomic vapor density 1.7×10^{17} cm^{-3}, assuming no hfs. No atom-wall interaction is considered ($C=0$) and the ratio of homogeneous to Doppler width is $\gamma_{12}/ku\approx16$. The thicker solid line is for an exponentially decaying field theory, the dashed line is results for a uniform electric field. The light line results from using the steady state, complex index of refraction of the vapor.

For $N<1\times10^{15}$ cm^{-3} the field attenuation is small, and does not change the SR line shape significantly. This small attenuation plays the same role as an imaginary convergence constant required in the Ducloy theory, and the low-density result is the same as from Refs. [1–3]. However, the strong, frequency-dependent field attenuation has a major influence at the higher N. Figure 4 shows that using an exponentially decaying field blueshifts the SR line shape compared to that obtained without attenuation. The result of using the steady-state complex index of refraction of the vapor, including collisional broadening but ignoring the wall transient and interaction, is also plotted in Fig. 4; this does not agree with either the SR approximation even at this high density. Also, notice that the ''center frequency,'' where the SR signal is midway between its maximum and minimum, is not at the atomic resonance, due to the contribution of the imaginary part of atomic polarizability (i.e., absorption), which is not negligible in the high density, even when the atom-wall interaction is neglected. This imaginary function, which is a Lorentz profile, is not equal to zero when field detuning is zero. So this contribution will shift the dispersion profile of SR signal to red. Multiple-component line effects will be considered in the next section, in the context of comparing to the present data.

IV. EXPERIMENTAL RESULTS AND DISCUSSION

The SR line shapes of the Rb D_1 line were measured for temperatures of 175 °C, 225 °C, 275 °C, 325 °C, 375 °C, 400 °C, and 425 °C. These data are given in Ref. [17], so only a representative set are reported here. It is first necessary to verify that the data were taken in the low-power limit, as optical pumping affects the SR line shape. The effect of optical pumping on SR has been studied for Rb vapor and Cs vapor, and a detailed theory has been given in Refs. [8,9]. It is most severe at low N, so we have tested for it by using the dependence of SR on intensity for the lowest N studied (3×10^{14} cm^{-3}). Details are given in Ref. [17]. The amplitude of the largest SR peak was most sensitive; it decreased

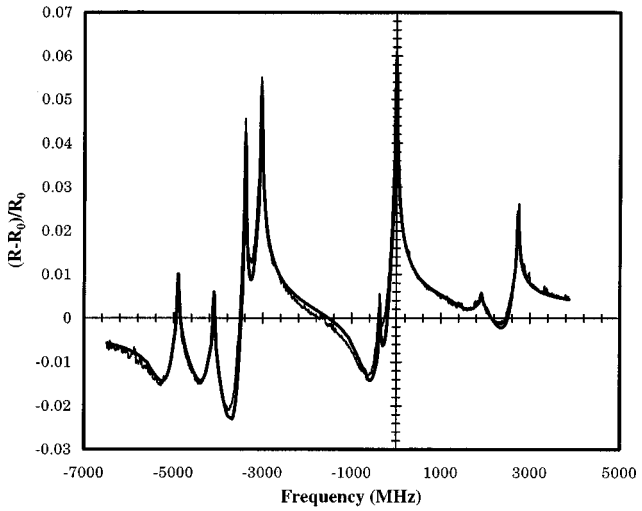

FIG. 5. The experimental SR line shape of Rb D_1 line and the theoretical fitting (smooth line) with convolution procedures with $C=0.20$ at $N=3\times10^{14}$ cm^{-3}.

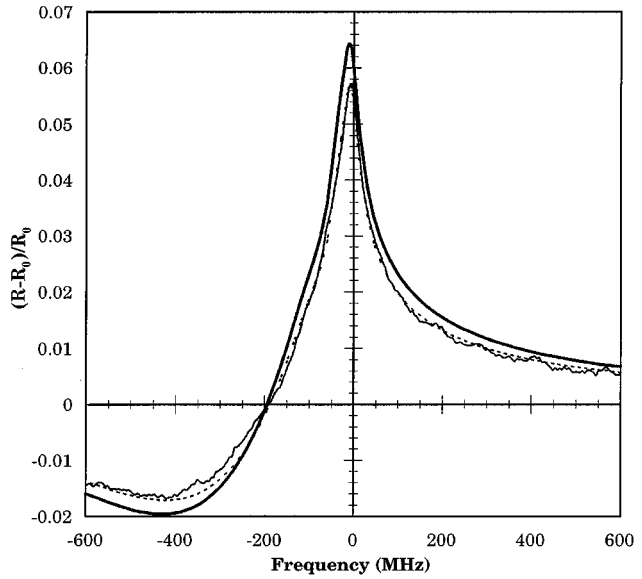

FIG. 6. The comparison of single line shapes of Rb^{85} $F=3\rightarrow F'=2$ from deconvoluted experimental data to the Ducloy's theory with $C=0.25$ (solid line) and $C=0.15$ (dashed line) at the density $N=3\times10^{14}$ cm^{-3}.

$\sim$1.6% from the zero-intensity limit at 0.6 mW cm^{-2}. All the experimental data following this section are acquired at that intensity.

In principle, Eqs. (8) and (9) can be used to calculate the full line shape for comparison to the data. This has been done for the higher N, but at the lowest densities it is very difficult to obtain convergence for detunings that are weakly attenuated. To overcome this, we concentrated on the largest peak, at zero detuning (Δ) in Fig. 5, for the lowest density studied (175 °C, $N=3\times10^{14}$ cm^{-3}). There is one strong and one weak hyperfine component in this spectral region. We assume that the line shapes of all eight components are the same and that the overlaps are weak at this low density, so that the SR intensities are additive (neglecting interference). Shurmanns' and Ducloy's low-density theories yield essentially the same, slowly varying SR intensity at large detunings. We assume that this is the correct far-wing line shape at these low densities, and use it to subtract the contributions of the six components whose resonances are far from $\Delta=0$. We then ''deconvolve'' the remaining signal as a sum of the two components near $\Delta=0$, using Fourier transform techniques. In this deconvolution the frequency and relative amplitude of each hyperfine component is known, and one is much weaker so the neglected interference is relatively minor. Figures 6 and 7 show the single-component experimental line shape obtained by this data deconvolution procedure, and the line shapes predicted by essentially the Ducloy theory [reduced Eqs. (8) and (9)] using different C parameters and vapor densities. In Fig. 6 the size of the theoretical peak value varies 4% as C increases from 0.15 to 0.25, and the position shifts 2–3 MHz. The peak height of the experimental line shape falls between the two theoretical curves with these C values, confirming the expected C value. However, it is redshifted $\sim$4 MHz from the $C=0.2$ theory (Fig. 7), and this is attributed to collisional plus Lorentz-Lorenz shift. The peak value and the linewidth change, by 12% and 15%, respectively, when N is increased by 17%, allowing clear verification of the expected density. This comparison shows that at low density the full experimental line shape matches well with the theoretical line shape for the expected values of N and C. Ducloy has previously tested this theory using a modulation technique that emphasizes the line core, and demonstrated good agreement [10].

With increasing density, the interferences between reflected electric fields of different hyperfine components must be included, but the attenuation is still small when the frequency is detuned a few γ_{12} from resonance with any hyperfine structure component, so that the full calculation was still excessive. Thus, we have approximated the SR signal as the weighted sum of the eight components, as in Eq. (9), but using a $\Phi(\Delta_n)$ that is the same for each component. This $\Phi(\Delta)$ is obtained using a single-component $\alpha(\Delta)$ in Eq. (8); overlapping absorptions are neglected. An example of this fit to the data is given in Fig. 8, where the theoretical curve has been shifted -85 MHz to match the experiment. This shift is again attributed to the sum of Lorentz-Lorenz and collisional shift. The discrepancies are due to using an incorrect $E(\Delta,z)$ in the calculation, compounded by assuming that all components have the same $\Phi(\Delta)$, which ignores overlapping absorptions. We tested different values of C in these intermediate density calculations, without significant improvement, concluding as above that $C=0.2\pm0.05$. Ducloy initially found a value of C_3 that was a factor of 2 higher than expected for the Cs D_1 transition [8], but with improved accuracy agreement was later reported [10], as we find here for Rb.

As N rises further, collisional broadening increases, the interference between components becomes strong, and $\alpha(\Delta)$ involves overlapping attenuations. However, the attenuation is now large enough to allow a full overlapping-attenuation calculation of Eqs. (8) and (9) within a reasonable computational time. Figure 9 shows the experimental data at $N=3.6\times10^{16}$ cm^{-3} and the theoretical fit using Eqs. (8) and (9) with multiple-component, steady-state, exponential attenuation of the field. Of course, the latter two assumptions as well as the Lorentz-Lorenz field correction and collisional

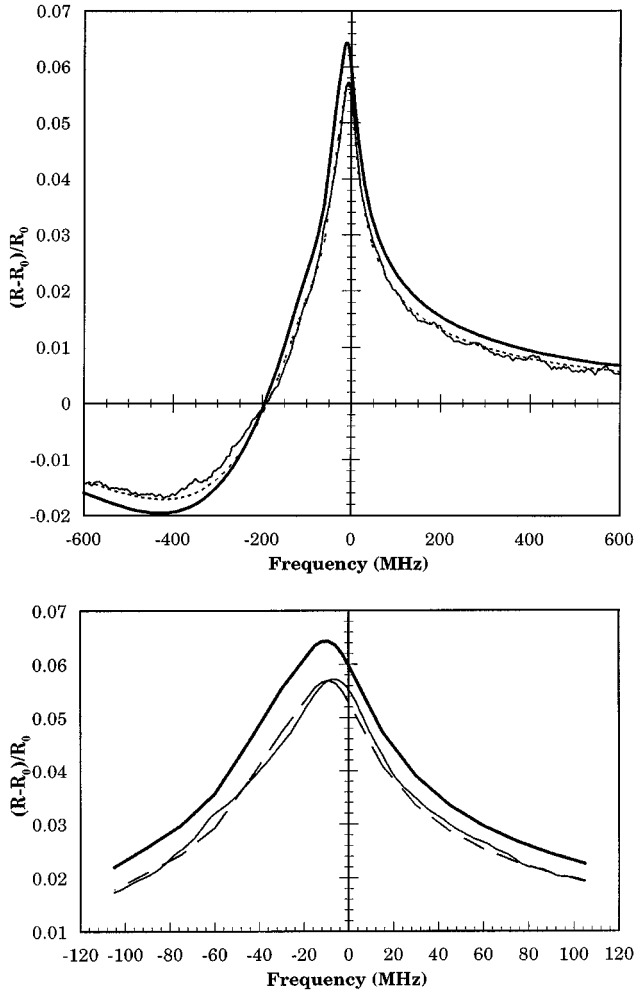

FIG. 7. The comparison of single line shapes of Rb^{85} $F=3\rightarrow F'=2$ from deconvoluted experimental data to the Ducloy's theory with $C=0.20$ at the density $N=3\times10^{14}$ cm^{-3} (dashed line), and $N=3.5\times10^{14}$ cm^{-3} (solid line). (a) The full single line shape of SR, (b) the peak of SR.

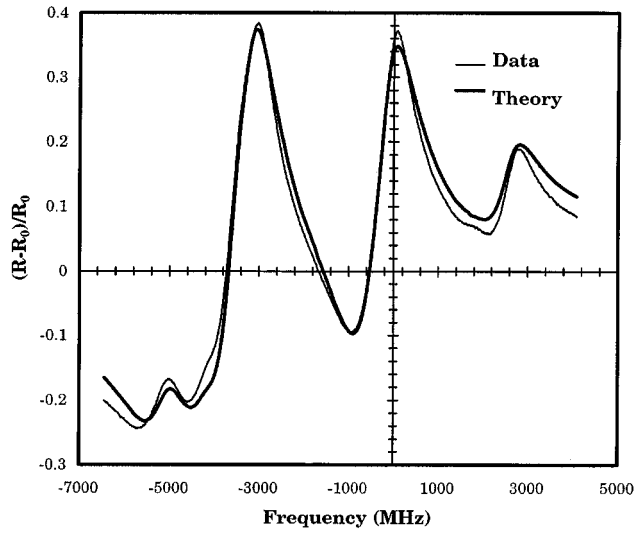

FIG. 8. Experimental data and theoretical fitting with convolution procedures at the number density of $N=8.6\times10^{15}$ cm^{-3}.

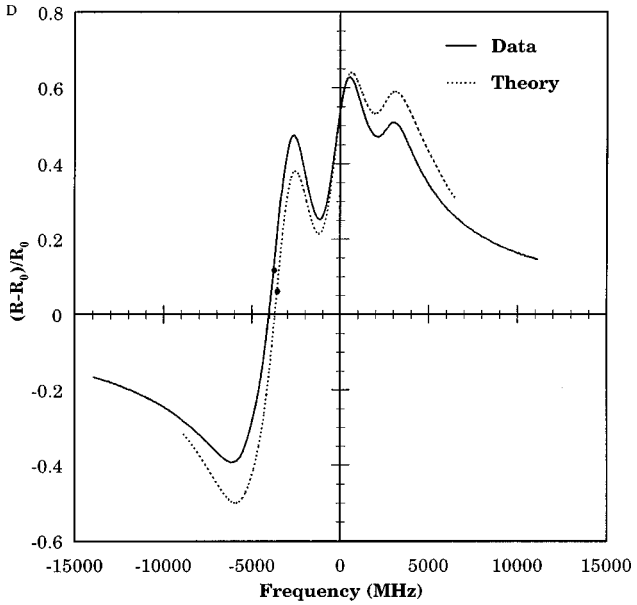

FIG. 9. The experimental data and the theoretical calculation with consideration of the interference between component fields at moderate density $N=3.6\times10^{16}$ cm^{-3}.

shift cause divergence from the experiment, as seen in Fig. 9. The black dots in Fig. 9 are the points midway between the maximum and minimum of each SR line shape. The frequency difference of the two black spots is 380 MHz and the difference between theoretical and experimental line shapes is 350 MHz at zero crossing points. Thus it appears possible to assign an approximate value to the Lorentz-Lorenz plus collisional shift at this density, using these theoretical approximations.

The collisional broadening full width at half maximum (FWHM) is ~7 GHz at $N=1.0\times10^{17}$ cm^{-3}, which is about the size of the entire hfs of the Rb D_1 line and yields a single-peaked, dispersionlike line shape. The experimental line shapes of SR are plotted in Fig. 10 for $N=1.0$, 1.7,

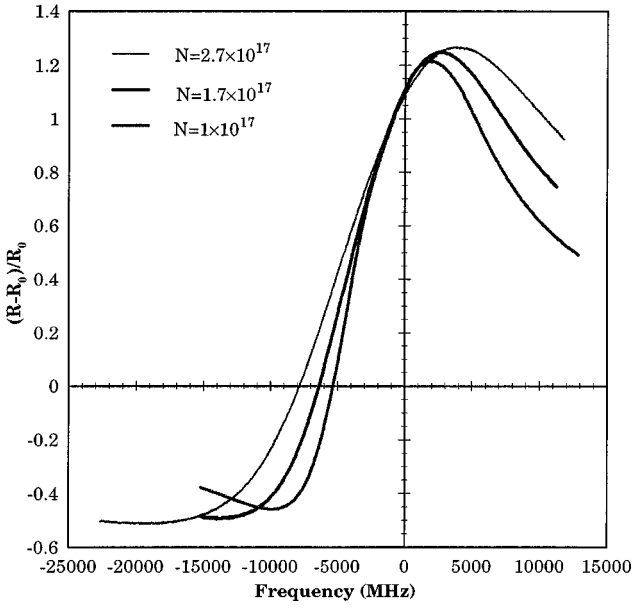

FIG. 10. The experimental data at high vapor density.

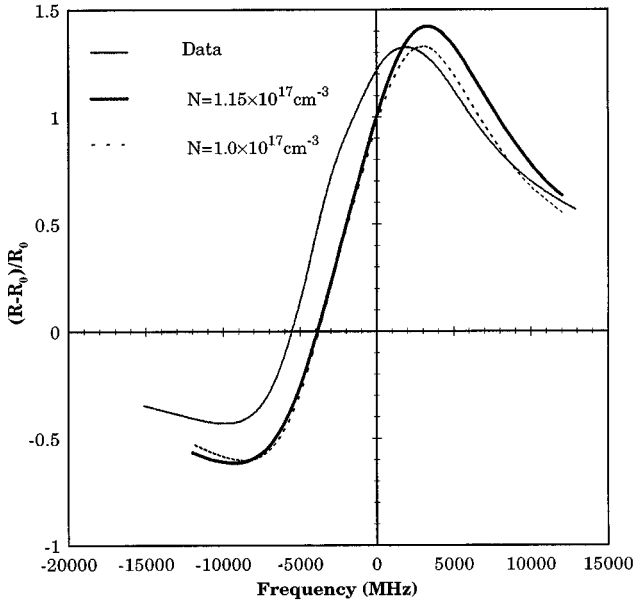

FIG. 11. Comparison of the experimental data to theoretical calculations of the SR line shape using vapor densities of $N=1.0\times10^{17}$ cm^{-3}, and $N=1.15\times10^{17}$ cm^{-3}.

and 2.7×10^{17} cm^{-3} (according to the Langmuir-Taylor relation). At high density the multiline theory converges quickly due to the strong attenuation (<1 μm) and the large homogeneous width. In Figs. 11 and 12 the theoretical SR line shapes are compared to the observations, again with $C=0.2$. In Fig. 11 different values of N are tested, leading to the conclusion that 1.15×10^{17} cm^{-3} fits better than $N=1.0\times10^{17}$ cm^{-3} predicted by the Langmuir-Taylor relation at 375 °C. We conclude that, at high density as well, the accuracy of N from the experiment is better than $\pm20\%$.

We have so far assumed that the theoretical line broadening rate coefficient (k_{br}) is correct and independent of density. Experiments at much lower densities have been consistent with this (Ref. [13], and references therein); here we have tested it at higher N, and found agreement within $\pm5\%$.

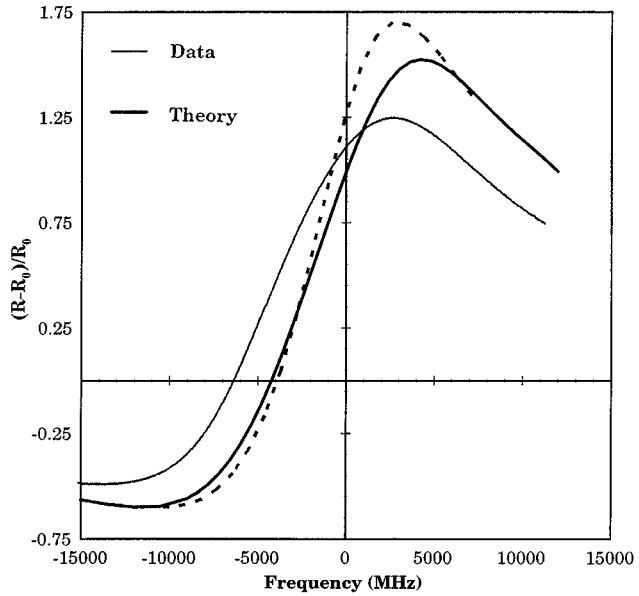

FIG. 12. The comparison of the experimental data and the theoretical calculation of the SR line shape at $N=1.7\times10^{17}$ cm^{-3}.

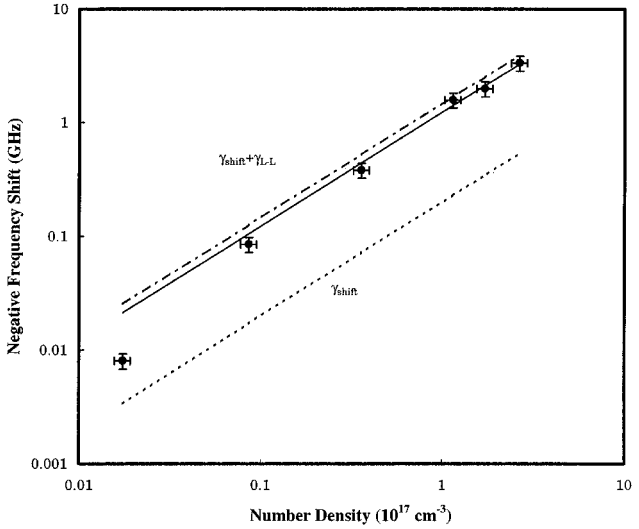

FIG. 13. Measured frequency shifts of SR line shape (dot), total theoretical redshift including Lorentz-Lorenz redshift (dot dashed line), and collisional shift (dashed line). The solid line is a $\Delta\nu\propto n$ fit to the experimental high-density data.

The peaks of the theoretical line shapes are higher than those from the experiment, and the line is shifted. If the Lorentz-Lorenz correction is approximated as a simple shift, we obtain 1.57, 1.97, and 3.33 GHz at $N=1.0$, 1.7 and 2.7×10^{17} cm^{-3} for this plus the collisional shift, using the shift of the points midway between the maximum and minimum of each SR, as shown in Fig. 10. This is only a best estimate; a full theory must use a self-consistent field including the Lorentz-Lorenz correction at each Δ. Probably the largest error of the present calculation is using the steady-state absorption coefficient, as the actual absorption is modified by the transient-field effect near the wall.

V. COLLISIONAL SHIFT, LORENTZ-LORENZ SHIFT, AND TRANSIENT SHIFT OF Rb D_1 LINE

The collisional shift and Lorentz-Lorenz shift are features of the interaction of identical atoms in an atomic vapor. The wall interaction redshifts the SR peak [8] and a blueshift results from a spatial oscillation of the amplitude of the transmitted field near the wall when the field is obtained self-consistently [13], SR offers the potential of measuring each or combinations of these shifts, and we summarize our data here. As described above, approximate theoretical line shapes have been compared to the data to obtain total shifts versus N. For $N<10^{16}$ cm^{-3} the SR peak is narrow and we have used its shift, while at higher N the shift of the mid-height position is a better measure (as in Fig. 9). These apparent total shifts between the experimental and theoretical SR spectra are given in Fig. 13. The indicated uncertainties primarily represent data-theory fitting uncertainties, as previously described. However, a slight scanning nonlinearity also contributed a few percent uncertainty at some densities. The atom-wall interaction is included in this theory, but the collisional shift, the Lorentz-Lorenz correction, and the transient shift (due to field alternation or oscillation in the self-

consistent manner [13]) are excluded.

The theoretical collisional shift from Ref. [21], plus the Lorentz-Lorenz shift ($\gamma_{L\text{-}L}$) are plotted in Fig. 13, where we have used $\gamma_{L\text{-}L}=-(1/3)fr_e\lambda cN=-(\pi/3)Nk^{-3}\Gamma$. For the Rb D_1 line, without consideration of hfs components, $\lambda_{L\text{-}L}/2\pi=-1.26\times10^{-8}\ N\ \text{cm}^3\,\text{Hz}$. The theoretical collisional shift is about $-0.20\times10^{-8}\ N\ \text{cm}^3\,\text{Hz}$, and this is not affected by hfs since the inverse of the collision time is greater than the hfs splitting. The sum of these theoretical shifts, divided by N, is $k_{\text{Sh}}=-1.46\times10^{-8}\ \text{cm}^{-3}$, while the data for $N\geqslant10^{16}\ \text{cm}^{-3}$ fits $k_{\text{Sh}}=-(1.22\pm0.24)\times10^{-8}\ \text{cm}^{-3}\,\text{Hz}$, where the uncertainty of $\pm20\%$ is primarily due to the uncertainty in the determination of atomic number density at high temperature. Within experimental uncertainty, this theoretical total shift agrees with the data at $N\geqslant10^{16}\ \text{cm}^{-3}$.

The point at $N=1.7\times10^{15}\ \text{cm}^{-3}$ is much lower than the $k_{\text{Sh}}=-1.46\times10^{-8}\ \text{cm}^{-3}$ line in Fig. 13, and we can qualitatively explain this as follows. At low N the eight hyperfine components of the D_1 line are grouped into four isolated, Doppler-broadened components. Only the fraction of the oscillator strength in one component contributes to the dipole, which causes the Lorentz-Lorenz shift of this component. Thus, $\gamma_{L\text{-}L}$ is reduced by this fraction, which is reasonably consistent with the data. That $\gamma_{L\text{-}L}$ at $N\leqslant10^{16}\,\text{cm}^{-3}$ is not reduced further is rather surprising. Only a fraction $g_{21}/\Delta w_D$ of the atoms in one Doppler component are excited to an upper state when illuminated by narrow-band radiation at low vapor density, and a corresponding reduction in $\gamma_{L\text{-}L}$ might be expected as was suggested by Ref. [21]. However, Ref. [12] recently showed theoretically that this reduction does not occur for an isolated line. The shift of different components that overlap within a Doppler envelope are more complicated [12], but the transition we investigated in Fig. 6 is the dominant component of that isolated line component, and should behave nearly as an isolated hfs component. The data agree with the Guo *et al.* result, as we measured a shift of 8 ± 1 MHz, whereas including the additional reduction factor of $\gamma_{21}/\Delta\omega_D$ yields 1 MHz.

VI. DISCUSSION OF SHIFTS

The collisional shift was theoretically predicted by Cooper and Stacey [21]. The ratio of $\gamma_{\text{shift}}/\gamma_{\text{self}}$ for $J_e=\frac{1}{2}\rightarrow J_g=\frac{1}{2}$was calculated to be -3%. Recently, the collisional shift of the Cs D_1 line was measured by Vuletic *et al.* [16] from SR at low vapor density, and their measured value of $\gamma_{\text{shift}}/\gamma_{\text{self}}$ is about -12% with an error up to 50%. The result is obtained by taking the average of the frequencies of the SR line-shape maximum and minimum as the atomic resonance center in the dispersionlike line shape. However, several other contributions to the shift occur and were not accounted for. These are the transient shift, the Lorentz-Lorenz shift, and interference between hyperfine components, as identified in [12]. The latter effect is also indicated by the different shifts reported for different hfs components of CS [23].

A measurement of the collisional shift plus the Lorentz-Lorentz redshift of potassium has been reported by Maki *et al.* [15], based on high-density shift data. They considered the frequency of the point midway between the maximum and the minimum of the SR line shape as the line-center frequency, and the shift of this frequency relative to an isolated atom as the frequency shift. This neglected a major correction due to the SR line-shape shift caused at high density by the imaginary refractive index (i.e., absorption) of the atomic vapor. A second problem was assuming that the wall interaction becomes negligible at high N, as we have shown it cannot be neglected at any N. Finally, the transient shift was also not known at that time. Thus, we believed that this is also an incorrect result for the collisional plus Lorentz shifts.

Here we have measured $\gamma_{\text{shift}}+\gamma_{L\text{-}L}+\gamma_{\text{trans}}$ by using a relatively complete theoretical interpretation of our data. We take into account the atom-wall interaction, which introduces a redshift, the wall transient that produces a blueshift, the superposition of fields from different hfs components, and for the higher N we include an exponentially decaying field. γ_{trans} is an additional blueshift expected to occur when a self-consistent field [9] is used. From the high-density data a ratio $(\gamma_{\text{shift}}+\gamma_{\text{trans}}+\gamma_{L\text{-}L})/\gamma_{\text{self}}=-0.180\pm0.035$ is obtained for Rb D_1 line. The theoretical values of $\gamma_{L\text{-}L}/\gamma_{\text{self}}$ is -0.185 and hence $(\gamma_{\text{trans}}+\gamma_{\text{shift}})/\gamma_{\text{self}}$ is about 0.05, so it appears that oscillation-field-induced transient and collisional shifts have roughly the same amplitude, but different signs.

VII. CONCLUSION

Selective reflection was first observed at the beginning of the century, but it remains a complicated phenomenon for atomic physics theory. A seemingly simple SR experiment may involve many physical processes that are interleaved in the observations, making it a challenge to obtain an accurate theoretical model. The theories of SR prior to Guo *et al.* assumed very small attenuation of the incident light, or low vapor density (N), and single component lines. The full SR line shape had not been accurately tested even for this limiting condition. That has been done here, and we found it satisfactory to explain our low-N data once hfs interferences were properly accounted for. The theory of SR is given here for multiple-component lines, at low or high density, and including the atom-wall interaction as obtained by Ducloy. However, we approximate the field attenuation as exponential, with the attention coefficient that of the steady-state vapor in the region away from the wall.

A comparison has been made between single-component line shapes with and without atom-wall interaction, or exponential attenuation of the field, and versus N. When the atom-wall interaction is included, the peak value of SR increases while the linewidth narrows and redshifts. When exponential attenuation is included, at moderate to high N, the SR line shape changes and a blueshift occurs. Comparing the data and theory for different N indicates that N can be determined within $<20\%$ using SR data, although a self-consistent-field theory is needed to take full advantage of this potential at high N.

Overlapping hfs components do not have a simple consequence; this has been taken into account here by including the interference between the multiple reflected-field components. However, at intermediate N, our approximation ignored the effect of overlapping-line contributions to the attenuation of the incident light. In addition, a correct theory requires a self-consistent calculation of the incident light at-

tenuation and the reflected fields. At high N we found considerable discrepancy between the calculated and measured SR line shapes due to this absence of a self-consistent field. Such a calculation has been performed by Guo *et al.* in Refs. [12–14], but not for the full complexity of the present D_1 line at many densities.

The atom-wall interaction significantly changes the line shape of SR and is not negligible at any vapor density. The surface attraction strength C_3 of London–van der Waals potential of Rb D_1 line is calculated as 1.2 kHz mm^3 using a hydrogenic (quantum defect) model for the atomic properties. The validity of this calculation has been verified by comparing low-N data to theory.

The sum of the collisional plus Lorentz shift plus self-consistent-field-induced transient shift has been obtained versus N, although the accuracy was limited at high N by the lack of a self-consistent-field, overlapping-line calculation. Within this accuracy, the data agreed with the calculated shifts. However, the collisional shift is a very small fraction of the total shift, so it is essentially undetermined in this experiment. (We do not believe it has been determined in any other experiment either.) A careful analysis of low-N data confirmed the absence of a reduction in the Lorenz-field shift corresponding to the ratio of the homogeneous to Doppler width. However, the data yielded the expected reduction due to isolated hyperfine line components.

For this SR experiment, a challenging problem was to build a corrosive-resist apparatus for high alkali vapor density. A robust Rb vapor cell, composed of kovar, sapphire window, and polycrystalline alumina, was designed and made using a sealing frit. A Rb density as high as $N=2.7\times10^{17}$ cm^{-3} has been studied using this setup, and it has been operated with Rb vapor in the temperature range of 325 °C–425 °C for more than 500 h without leakage.

ACKNOWLEDGMENT

This work was supported by NSF Grant No. PHY90-12244.

[1] J. P. Woerdman and M. F. H. Schuurmans, Opt. Commun. **14**, 248 (1975); M. F. H. Schuurmans, J. Phys. (France) **37**, 469 (1976); A. L. J. Burgmans and J. P. Woerdman, *ibid.* **37**, 677 (1976).

[2] V. L. Velichanskii, R. G. Gamidov, G. T. Pak, and V. A. Sautenkov, Pis'ma Zh. Eksp. Teor. Fiz. **52**, 176 (1990) [JETP Lett. **52**, 136 (1990)].

[3] A. M. Akul'shin, A. A. Celikov, V. V. Sautenkov, T. A. Vartanian, and V. L. Velichansky, Opt. Commun. **85**, 21 (1991).

[4] V. Vuletic, V. A. Sautenkov, C. Zimmermann, and T. W. Hansch, Opt. Commun. **108**, 77 (1994).

[5] O. A. Rabi, A. Amy-Klein, S. Saltiel, and M. Ducloy, Europhys. Lett. **25**, 579 (1994).

[6] T. A. Vartanyan and F. Trager, Opt. Commun. **110**, 315 (1994).

[7] P. Simoneau, S. Le Boiteaux, Cid B. De Araujo, D. Bloch, J. R. Rios Leite, and M. Ducloy, Opt. Commun. **59**, 103 (1986).

[8] M. Chevroller, M. Fichet, M. Oria, G. Rafmat, D. Bloch, and M. Ducloy, J. Phys. (France) II **2**, 631 (1992).

[9] G. Nienhuis, F. Shuller, and M. Ducloy, Phys. Rev. A **38**, 5197 (1988).

[10] M. Ducloy and M. Fichet, J. Phys. (France) II **1**, 1429 (1991).

[11] R. P. Srivasta and H. R. Zaidi, J. Quant. Spectrosc. Radiat. Transf. **16,** 301 (1976).

[12] J. Guo, J. Cooper, A. Gallagher, and M. Lewenstein, Opt. Commun. **110**, 732 (1994).

[13] J. Guo, A. Gallagher, and J. Cooper, Opt. Commun. **131**, 219 (1996).

[14] J. Guo, J. Cooper, and A. Gallagher, Phys. Rev. A **53**, 1130 (1996).

[15] J. J. Maki, M. S. Malcuit, J. E. Sipe, and R. W. Boyd, Phys. Rev. Lett. **67**, 972 (1991).

[16] V. Vuletic, V. A. Sautenkov, C. Zimmermann, and T. W. Hansch, Opt. Commun. **99**, 185 (1993).

[17] Ping Wang, Doctoral thesis, University of Colorado, 1995 (unpublished).

[18] J. A. Neuman, P. Wang, and A. Gallagher, Rev. Sci. Instrum. **66**, 3021 (1995).

[19] J. B. Taylor and I. Langmuir, Phys. Rev. **51**, 753 (1937).

[20] A. Gallagher and E. L. Lewis, J. Opt. Soc. Am. **63**, 864 (1973).

[21] J. Cooper and D. N. Stacey, Phys. Lett. **46A**, 299 (1973).